JOURNAL OF Applied Polymer SCIENCE

Effects of Substrate Composition and Roughness on Mechanical Properties and Conformality of Parylene C Coatings

Adrian Verwolf, Grady White, Chris Poling
National Institute of Standards and Technology, Materials Reliability Division, MS 653 Boulder, Colorado 80305

Correspondence to: A. Verwolf (E-mail: adrian.verwolf@sundropfuels.com)

ABSTRACT: Nanoindentation was used to determine reduced elastic modulus E_r and hardness H of 16 μm thick Parylene C coatings vapor-deposited on mill-finished samples of aluminum, copper, nickel steel, and stainless steel. Profilometry was used to compare average surface roughnesses of the polymeric coatings to the roughnesses of the underlying metals, thereby providing a quantitative index for determining conformality. Roughness, elasticity, and hardness of coatings were found to be affected by both chemical composition and surface roughness of four different metallic substrates. Standard nanoindentation evaluations of E_r and H distributions for the various metals were found to be positively skewed, which precluded use of simple averages for purposes of comparison. However, analysis of the nanoindentation and profilometry data by use of alternative techniques indicated that coatings were consistently smoother and flatter than their underlying substrates, i.e., they were not truly conformal, and nanomechanical properties of Parylene C were affected by the chemical composition of the substrates independently of the effects of substrate roughness.
 J. Appl. Polym. Sci. 000: 000–000, 2012

KEYWORDS: Parylene C; nanoindentation; modulus; hardness; conformal

Received 12 September 2011; accepted 24 April 2012; published online
DOI: 10.1002/app.37972

INTRODUCTION

Reported attributes of poly(chloro-para-xylylene), known commercially as Parylene C, e.g., low water permeability,[1] large strain to failure and biocompatibility,[2] room-temperature conformal coating deposition process,[3] and compatibility with steam autoclave, ethylene oxide, or γ-irradiation sterilization techniques,[4] meet critical requirements for use in implanted medical devices. Parylene C is presently approved by the US Food and Drug Administration as a coating for certain temporarily implanted medical components such as electrical leads. Because Parylene-coated electrical leads as well as next-generation passive and active implanted medical devices will be subject to flexing and other stresses inside the body, baseline work to assess the reliability of Parylene C as a conformal barrier coating comprises, in part, measuring the mechanical properties and uniformity of the film. Once mechanical reference values are determined, degradation mechanisms and rates must be identified and understood before Parylene C, which can be used as a barrier coating on chronically implanted devices. Moreover, development of quantitative test procedures to assure reliability is critical for attaining regulatory approval. However, before accelerated failure tests can be developed or interpreted, a thorough understanding of both average values and variability of relevant material properties of as-deposited Parylene must be evaluated. To this end, nanoindentation determinations of elastic response and hardness of Parylene C on a variety of substrates were made and are reported. Further, profilometric measurements of both Parylene-C-coated and uncoated samples were taken to provide comparative measurements of surface roughness.

Nanoindentation consists of pressing a hard tip of known geometry into the surface of a material and then withdrawing the indenter tip while continuously measuring applied load P and tip vertical displacement h. The reduced elastic modulus (E_r) is defined by the relation[5]

$$\frac{1}{E_r} = \frac{(1-\nu_s^2)}{E_s} + \frac{(1-\nu_n^2)}{E_n}. \quad (1)$$

E_s and E_n are the specimen and load frame Young's modulus values, respectively, and ν_s and ν_n are the corresponding Poisson

Applied Polymer SCIENCE

ratios. E_r is calculated from the resulting load-displacement curves by use of equation[5]

$$E_r = \frac{\sqrt{\pi}}{2}\frac{S}{\sqrt{A}}, \quad (2)$$

where S is the stiffness, taken as the slope dP/dh of the unloading curve evaluated at the maximum load P_{max}, and A is the projected contact area of the indenter tip onto the specimen surface. Hardness H is calculated as

$$H = \frac{P_{max}}{A}. \quad (3)$$

A is an experimentally determined function of contact depth h_c, where h_c is determined as follows from P_{max}, maximum displacement h_{max}, S, and ε:

$$h_c = h_{max} - \varepsilon \cdot \frac{P_{max}}{S}; \quad (4)$$

ε is a factor used to account for tip geometry and is equal to 0.75 for a Berkovich tip. The preceding analysis technique accounts strictly for elastic-plastic deformation but considers no viscoelastic effects. Currently, there appears to be little information in the literature regarding values or variability of E_r and H for Parylene C. However, there is some evidence that the chemical composition of the substrates to which Parylene C is applied may substantially affect the structure and thickness of the coating.[6] The present work investigates substrate effects to establish nanoindentation reference data for unstressed Parylene C applied to a variety of flat, mill-finished metal substrates with average surface roughness $S_a < 1$ μm.

EXPERIMENTAL

Samples of 6061 aluminum alloy, copper, and 304 stainless steel were sheared from 0.32 cm-thick sheet stock into 25 mm by 51 mm rectangles for coating with Parylene C. Circular steel disks (#7620, SPI Supplies, West Chester, PA) 15 mm in diameter by 0.9 mm thick were also purchased commercially and included in the coating run. The rectangular samples were sonicated in a dilute degreaser solution (Micro-90, Cole Parmer, Vernon Hills, IL) for 15 min before being rinsed sequentially in reagent-grade acetone and reagent-grade ethanol and then being allowed to dry at ambient conditions for 24 h. The steel disks were used as received. All rectangular samples had a mill finish. The copper and aluminum samples showed some visible discoloration after sonication in the detergent, while the stainless samples were not visibly affected. Parylene coating was performed commercially (Specialty Coating Systems, Indianapolis, IN). A target thickness of 15 μm was specified; the run data sheet accompanying the finished order reported an average thickness of 16.13 μm for the set of coated samples. Samples were stored in closed steel that can limit environmental and light exposure.

Ambient temperatures during storage and testing ranged from 19 to 22°C. Reported values for Parylene C's glass transition temperature T_g vary from 35 to 150°C.[3,7,8] However, differential scanning calorimetry performed on ~10 mg samples from this coating run using a commercial instrument (TA Instruments DSC Q10, New Castle, DE) could not confirm this. The instrument exhibited a characteristic, sample-independent curve during heating from ambient conditions that precluded reliable measurement below 45°C. None of the samples exhibited a discernible transition between 45 and 100°C at a heating rate of 10°C/min. A similarly indeterminate result was observed previously.[9]

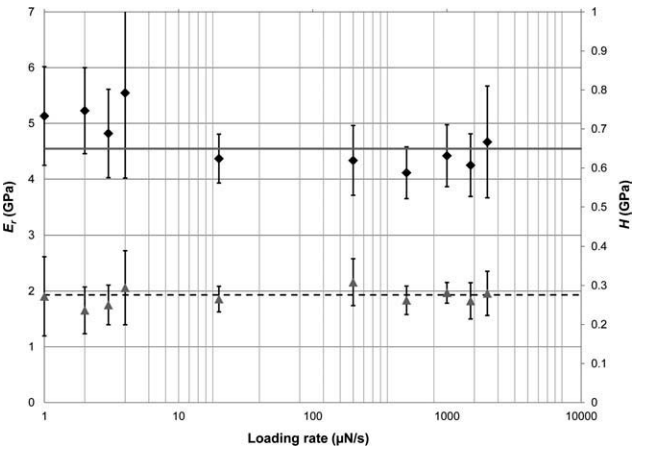

Figure 1. Plots of average E_r and H as functions of loading rate for Parylene C vapor-deposited directly on nickel steel mounting disks. Error bars on the points represent ±1 standard deviation. The upper solid line and lower dashed line are the weighted averages of E_r and H measurements, respectively, for loading rates from 4 to 2000 μN/s, inclusive. A loading rate of 200 μN/s was used for subsequent testing.

All rectangular samples were attached to uncoated steel disks with cyanoacrylate adhesive (Super Glue Corporation, Rancho Cucamonga, CA) prior to testing. The mounted samples as well as the Parylene-coated steel disks were held in place magnetically on the stage of a nanoindenter (Hysitron TI 900 TriboIndenter, Hysitron Corporation, Minneapolis, MN). An individual run consisted of a 5 × 5 grid of indentations spaced at 20 μm in both the x- and y-directions. Six such grids were arranged contiguously in a 3-by-2 pattern, with grids separated by 20 μm so as to maintain uniform spacing among all indentations. This pattern was repeated for each sample in a distinct location separated by several millimeters, yielding 300 indentations total for each sample. Individual 5 × 5 grids were chosen instead of a single 10 × 15 grid to better assess the run-to-run reproducibility of the sample-instrument system.

Prior to the conducting of this series of measurements, the instrument was calibrated in accordance with the instrument's operating manual to determine machine compliance and tip area function. Machine compliance was determined to be 0.35 nm/mN; the tip area function used was $A = 22.5h_c^2 + 1.36h_c$. Additionally, a z-axis force-displacement calibration was performed daily, again according to the manual, and a fused silica reference standard was indented as a calibration check prior to indenting each distinct region of six 5 × 5 grids. Scanning electron micrographs verified that the average circumscribed diameter of residual nanoindentation impressions was ~4 μm, consistent with the calculated value of 3.4 μm based on the

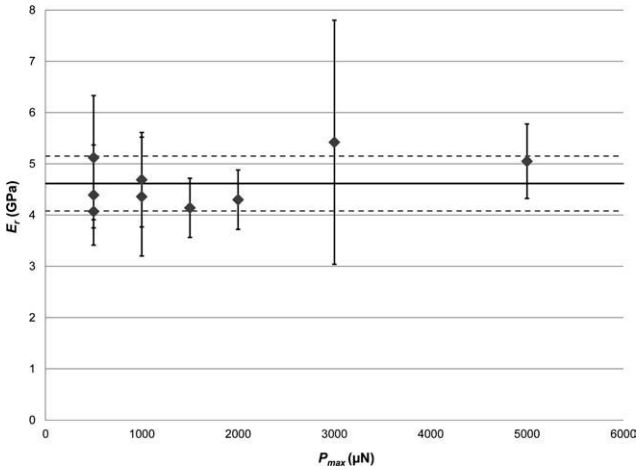

Figure 2. Plot of E_r as a function of peak load for Parylene C vapor-deposited directly on nickel steel mounting disks. Error bars on the points represent ±1 standard deviation. The solid line shows the weighted average of E_r for peak loads from 500 to 5000 μN, inclusive. Upper and lower dashed lines represent the 99% confidence interval about the average. Results for H were very similar which is not presented here. No significant variability in either E_r or H was observed as a function of P_{max}.

geometry of Berkovich indenter tip at a vertical displacement of 580 nm.

An initial study was conducted to identify potential effects of loading rate and peak load on the response of Parylene C. As shown in Figure 1, E_r and H did not vary significantly as the loading rate was increased from 4 to 2000 μN/s. Similarly, E_r data plotted in Figure 2 show that standard deviations overlapped for results obtained at peak loads between 500 and 2000 μN, inclusive. Given these results, peak load was set to 2000 μN to achieve 480 to 580 nm penetration depths, thereby reducing effects of the rounded, nonideal Berkovich indenter tip, which was estimated by the manufacturer to have a 150 nm radius of curvature. At the same time, these depths were less than 5% of the coating thickness, thereby avoiding substrate effects.[10,11] Samples were subsequently loaded and unloaded at 200 μN/s and held for 2 s at the peak load of 2000 μN. In all cases, the force threshold for determining initial indenter tip contact with the surface of the Parylene C was 3 μN.

A commercial profilometer (Ambios XP2 stylus profiler, KLA-Tencor, Milpitas, CA) was used to characterize the surface of all coated and uncoated samples. The stylus of the profilometer had a diamond tip with 2.5 μm radius. The load was 0.5 mg. To determine whether the profilometer was damaging the Parylene C surface, four repeated 2-mm scans were made on a Parylene coating deposited on a copper substrate. All scans showed identical surface profiles with identical amplitudes. Variability among the scans appeared to result exclusively from small (~3.3 nm) shifts in the reproducibility of the starting points for the scans. Profilometry measurements were taken on two different areas for each sample and on two samples for each substrate. Each area consisted of 21 parallel lines separated by 5 μm. There was one exception; the coated stainless steel consisted of 20 scan lines in each area. Each line was 500 μm long. The nanoindenter took a data point every 84.5 nm, where each data point was an average of instrument readings over that distance.

Qualitative tape peel tests were performed on both sides of individual samples that had been scored with a razor blade into square 5 × 5 grids measuring ~20 mm on a side. Cellophane tape (Scotch Multitask Tape, 3M Corporation, St. Paul, MN) was applied firmly to the grids and then peeled off at 90° relative to the surface of the sample. The force required to remove the pressure-sensitive tape from intact Parylene C was found to be (11.7 ± 1.4) N/100 mm of tape width by use of a servo hydraulic mechanical test frame with a 10 N force transducer (MTS 858 MiniBionix II, Eden Prairie, MN). None of the coatings delaminated from the substrate.

RESULTS

Examination of the load-displacement curves from which the hardness and elasticity values were calculated, and revealed that about 2.5% of measurements obtained were substantially different in profile. These indentations showed unusually large displacements at very low loads and were therefore excluded from the reported results. A typical load-displacement trace is shown in Figure 3.

Table I summarizes the data for Parylene C coatings on the four substrates. The values in Table I for the aluminum, copper, nickel steel, and stainless steel substrates were obtained by a simple average of all data. Values of E_r and H, as well as their standard deviations are given as well as the number of measurements that were made for each substrate material. In addition to the values obtained for Parylene C on the substrates of interest, data are also provided for the measurements made on the bare fused silica specimen. On the basis of results in Table I, it is not possible to discern any differences for E_r or H for Parylene C deposited upon the four substrates, although the standard deviation values for both steels were much larger than those

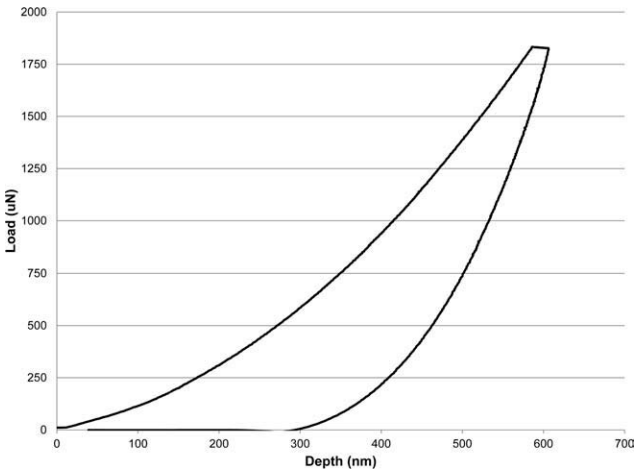

Figure 3. A load-displacement profiles for Parylene C. All of the profiles, including those that were excluded, had positive S values. The lack of a positively-sloped "nose" in the unloading portion of the curve, which can be pronounced when viscoelastic effects are substantial, provides some assurance that viscoelastic contributions did not induce gross error in the results.

Table I. E_r and H Values of Parylene C as Deposited on Different Mill-Finished Metal Substrates, with Values of the Uncoated Fused Silica Standard Collected Routinely to Assess the Measurement Stability of the Instrument

Substrate material	E_r (GPa)	H (GPa)	n
Aluminum	4.32 ± 0.58	0.26 ± 0.038	297
Copper	4.39 ± 0.69	0.26 ± 0.035	293
Nickel steel	4.40 ± 1.05	0.27 ± 0.070	288
Stainless steel	5.10 ± 1.87	0.33 ± 0.17	294
Fused silica standard	69.2 ± 0.75	9.48 ± 0.16	54

for the aluminum or copper substrates and those for stainless steel were much larger than those for the nickel steel substrates.

Figure 4, which plots histograms of the E_r values, shows that the data are positively skewed for all four substrates, and that the data for the stainless steel substrates are the most highly skewed. Similar results were observed for the H values, but are not shown here because of their qualitative similarity to the E_r data. The distribution of the E_r values means that simple averaging will bias the expected E_r to the right, away from the pronounced peaks shown in Figure 4, and the extent of the bias will be a function of the skew of the data. To address this issue, the histograms were fitted by Gaussian curves by use of a commercial program (Origin, OriginLab Corporation, Northampton, MA). This was done in two ways: fitting a Gaussian to all of the data and fitting a Gaussian to data in the vicinity of the peak while omitting the skewed data. Results for both E_r and H are shown in Figure 5.

For the fitting procedure resulting in Figure 5, all of the fit parameters were unconstrained for fits both to the censored data and to the complete data sets. The error bars represent the standard deviations of the peak positions. For E_r, censoring the skewed data does not change the fitted peak positions significantly. However, there is a clear difference between the E_r value obtained for Parylene C on the aluminum and copper substrates (~4.16 GPa) and that obtained on the two steel substrates (~3.98 GPa).

Except for Parylene on the stainless steel substrate, values of H in Figure 5 obtained on the censored data were indistinguishable from those using the complete histogram profiles. For the stainless steel substrate, the censored data value for H was about 0.01 GPa lower than that the values obtained on aluminum, nickel steel, or the uncensored stainless steel data. In contrast, both censored and uncensored data from the copper substrate resulted in an H that was roughly 0.02 GPa higher than that of the other substrates (and ~0.03 GPa higher than that obtained from Parylene C on the stainless steel substrate by the use of censored data).

Justification for using censored data to evaluate E_r and H depends critically on the reason for the skewed behavior.

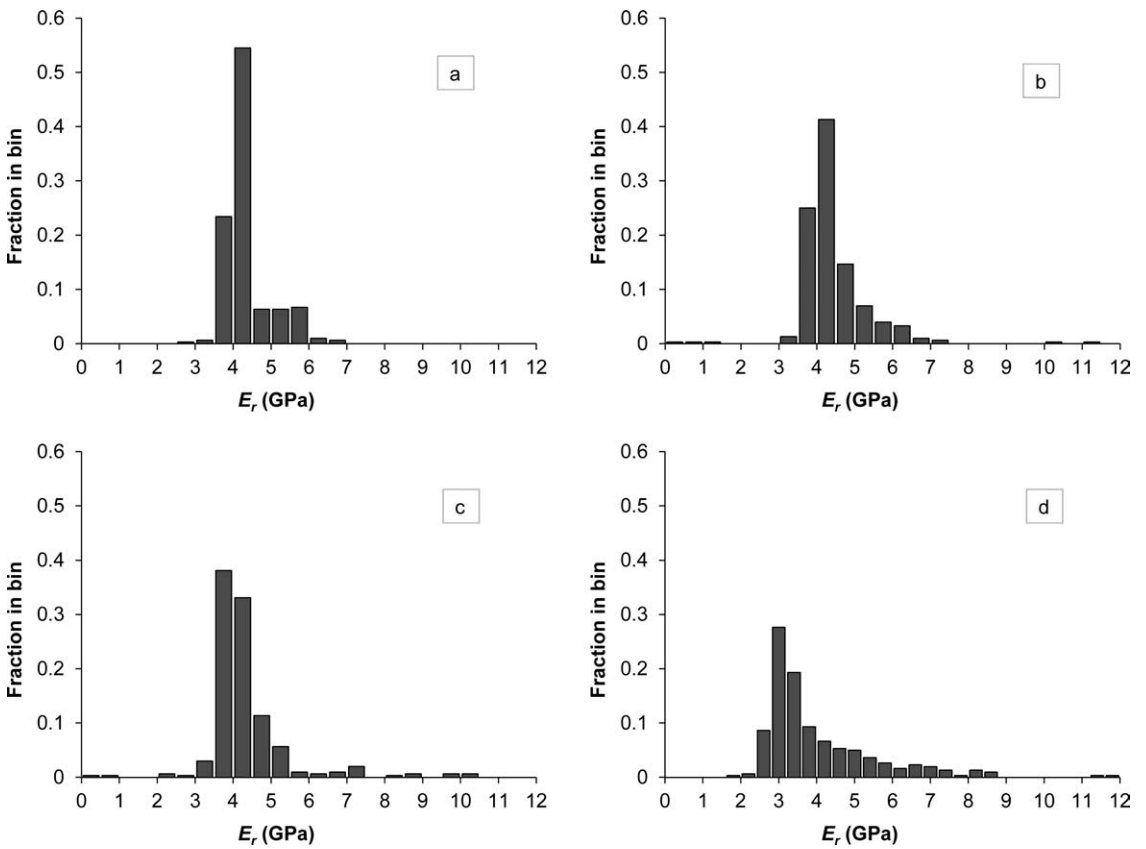

Figure 4. (a–d) Histograms of E_r for a Parylene C coating on (a) aluminum, (b) copper, (c) nickel steel, and (d) stainless steel. E_r and H for stainless steel had the largest skewness.

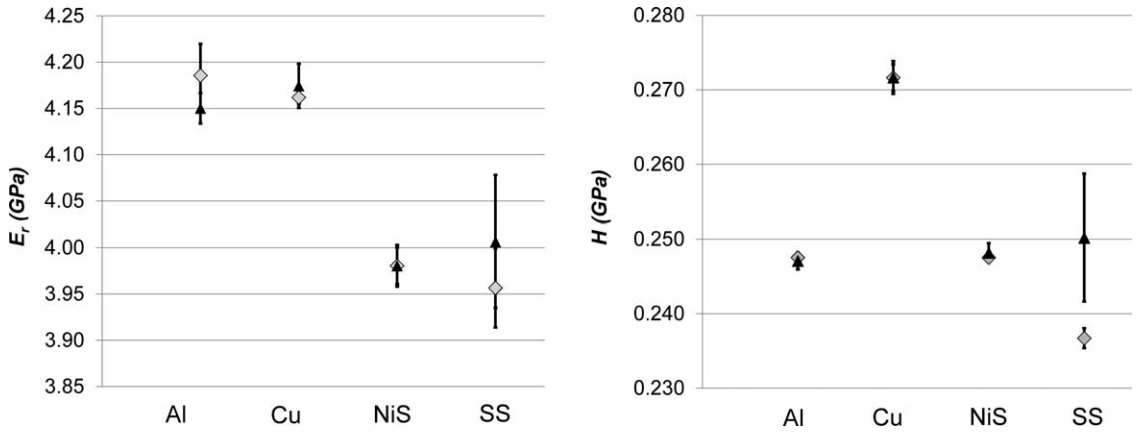

Figure 5. Peak positions obtained from Gaussian fits to the frequency distribution histograms (e.g., Figure 4) of E_r and H. Triangles are peak positions from fits to the entire distribution. Diamonds result from fits to censored data in which the data skewed to the right are not considered. Error bars represent ±1 standard deviation.

If both E_r and H have a naturally occurring skewed distribution, then censoring the data is not an appropriate course of action, and an asymmetric probability distribution should be used to analyze the entire data set. On the other hand, if the skewed behavior results from processes that are unrelated to material variations, then the observed positive skewness is likely to be an experimental artifact and censoring the data is reasonable. This issue will be discussed in Discussion Section. However, regardless of the source, with one exception, the standard deviations for censored and uncensored data overlapped for E_r and H.

The surface geometries of the bare and coated samples were evaluated using profilometry. As shown in the profilometry results of Table II, all Parylene C-coated surfaces were smoother and flatter than their uncoated counterparts, i.e., roughnesses and slopes, respectively, were lower for the polymer coatings than for the substrates to which they were applied.

Individual line scans were selected from the areal profilometry data so that linear surface profiles could be examined separately from the aggregate roughness and slope indices. Six lines from each coated and uncoated sample were selected (edge, center, and edge of each of the profiled areas) and divided into sequential segments consisting of integer multiples of the profilometer's average measurement interval (84.5 nm). The absolute value of slope $\Delta z/\Delta x$ along each x-segment (422, 1770, and 3550 nm) was calculated from each segment's endpoints. For comparison, the geometry of the Berkovich indenter tip yields slope values of 0.34 and 0.46, depending on which angles of the trigonal pyramid are used for the calculation. At the deepest penetration depth, the indenter-tip impression has a maximum linear distance on the specimen surface from the apex of the equilateral triangle impression to the center of the opposite side of ~3000 nm; the three distances chosen to calculate the slopes bracket this value.

Slope values were binned in intervals from 0 to 0.1 (exclusive), 0.1 to 0.2 (exclusive), 0.2 to 0.3 (exclusive), and 0.3 and greater. The number of points falling into each bin was divided by the total number of slope calculations along each line to obtain percentages. Results for individual lines were then aggregated for each substrate, as shown in Figure 6. Relative abundances of slopes <0.1 decreased with decreasing interval length for all samples. Taking Parylene-coated copper as an example, 85% of slope values were less than 0.1 for the 3550 nm interval, 82% were less than 0.1 for the 1770 nm interval (see Figure 6), and 78% were less than 0.1 at 422 nm. Conversely, percentages of slopes greater than or equal to 0.3 increased with decreasing interval size. The trend for coated copper is again typical of all samples: 0.23% for $\Delta x = 3550$ nm, 1.0% for $\Delta x = 1770$ nm (Figure 6), and 1.3% for $\Delta x = 422$ nm. Although this behavior is expected, the quantitative results are instructive in that the general trends and ranges of values are similar for all three Δx values. The single exception to this relationship was coated nickel steel, for which no slope ≥0.3 was observed at either the 1770 or 3550 nm Δx interval. Between slopes of 0.1 and 0.3, aluminum showed significant differences in both intervals due to coating, and stainless steel exhibited a significant reduction corresponding to the 0.2–0.3 and ≥0.3 intervals. The copper and nickel steel were statistically similar in that same range of slope values, as shown by the overlapping error bars in Figure 6.

Additional statistical comparisons were made at a 99% confidence level to determine whether coatings resulted in significant differences in surface slopes. Binned slope results from the six individual line scans were averaged and variance estimates calculated for coated and uncoated samples. F-tests (for variance) and t-tests (for means) were performed to provide a basis for comparing surface slopes from coated and uncoated samples of the same substrate material. Average slopes in all bins for coated and uncoated samples of aluminum and stainless steel were

Table II. Average Surface Roughness S_a and RMS Slope S_{dq} of Uncoated and Coated Metal Samples

	S_a (μm)		S_{dq}	
Substrate material	Uncoated	Coated	Uncoated	Coated
Aluminum	0.44	0.32	0.11	0.08
Copper	0.65	0.37	0.21	0.11
Nickel steel	0.39	0.20	0.14	0.10
Stainless steel	0.77	0.53	0.28	0.17

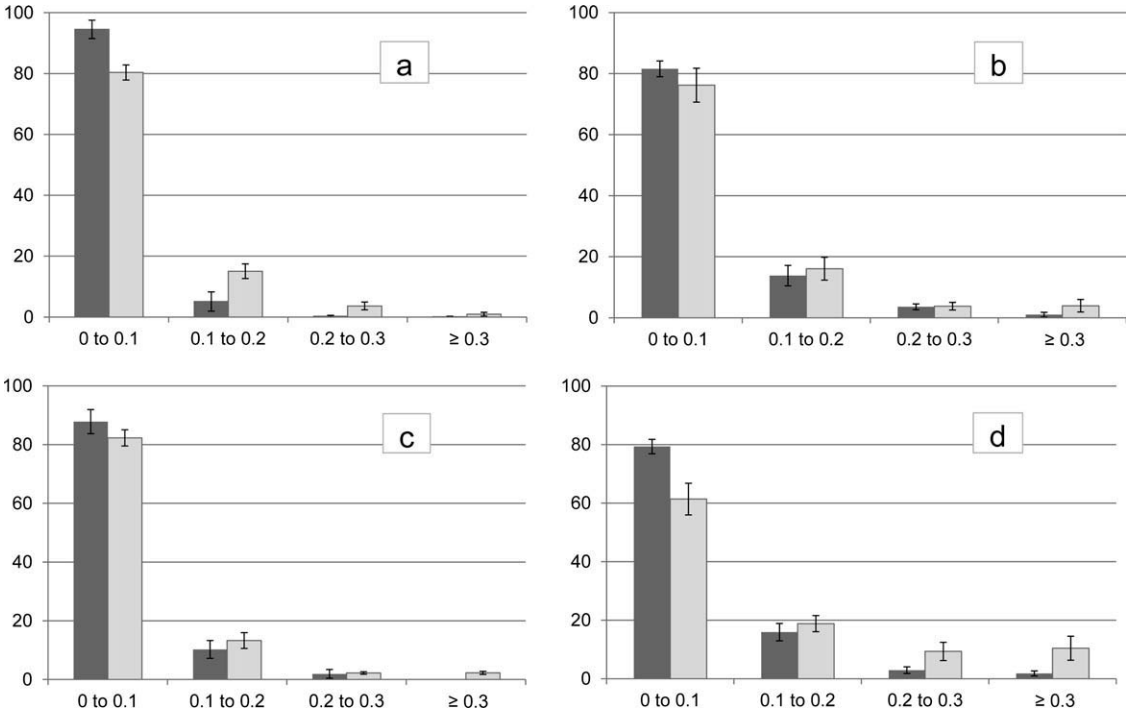

Figure 6. (a–d) Histograms of slope in percentages for (a) aluminum, (b) copper, (c) nickel steel, and (d) stainless steel samples. Darker, left-hand columns correspond to coated samples and lighter columns, to uncoated metals. Error bars indicate one standard deviation as calculated from six line scans. $\Delta x = 1770$ nm for all slope calculations shown, although similar results were obtained for $\Delta x = 422$ and 3550 nm.

different at a 99% confidence level, corresponding to a significant smoothing effect due to coating. Conversely, all binned slopes <0.3 for nickel steel and copper were accepted as having the same means, which indicates that the Parylene C induced no significant change in the smaller slopes for those metal substrates. However, slopes >0.3 were significantly different for copper and nickel steel. Though changes in low and intermediate slopes were not significant for all material substrates, coating with Parylene C significantly reduced the proportion of high slopes (≥0.3) for every metal tested.

A perfectly conformal coating, of course, would reflect the substrate exactly and yield very similar slope distributions for the substrate and the Parylene C. Apparent in Figure 6 is the tendency for all surfaces to become smoother upon coating, i.e., larger slopes (≥0.1) were reduced in all bins for all samples and smaller slopes (<0.1) increased for all samples. These changes were also true in all cases for the 422 and 3550 nm Δx segments. It should be noted that relative standard deviations for the 0–0.1 intervals were less than 5.5% for all samples, so good reproducibility was achievable with this testing system.

Though the coatings were smoother than the substrates, this effect did not result from weak polymer–metal interactions at the materials' interfaces. It was expected that Parylene C coatings could be readily peeled from the various substrates, particularly because no surface adhesion treatments were applied prior to deposition; however, the adhesive tape peel tests had no discernible effect on any square inscribed on any sample. In fact, removing even the smallest quantity of Parylene C from any of the samples required destructive scraping with a razor blade.

DISCUSSION

As shown in Table I, Parylene C deposited on a stainless steel substrate exhibited the largest variability in both E_r and H of all samples; aluminum and copper substrates were comparable and relatively low; and the nickel-steel mounting disks fell roughly in the middle of samples examined. However, based on the standard deviation values obtained from sample analyses in Table I, there is no significant difference among the E_r or H values for the different substrates. This is in clear contrast to the variations in both E_r and H with substrate that are determined from Gaussian fits to the frequency data and shown in Figure 5. The difference between the table and the figure raises two questions. What are the implications of fitting the distribution histograms to a normal distribution versus simply averaging the data? Is it reasonable to separate the skewed data from an expected symmetrical data distribution?

To address the first question, it must be noted that if the scatter in a data set is distributed symmetrically about the "true" value of the parameter being measured, a simple average of the data will give approximately the same value as that given by a fit to a symmetric distribution function, e.g., a Gaussian. The difference between the two values would reflect both the quality and the amount of the experimental data. As the amount of data increased, the difference between the average and the fitted peak position would be expected to asymptotically approach zero. For the measured values of E_r and H presented here, the data are not symmetric, and the mean will inherently be weighted by the positive outliers in the skewed distribution. In contrast, the fitted peak position of a symmetric distribution function will be

Table III. Values of E_r, H, and Average Surface Roughness S_a Derived from Gaussian Fits for Parylene C on Each Substrate

Substrate material	E_r (GPa)	H (GPa)	S_a (nm)
Aluminum	4.17 ± 0.05	0.247 ± 0.001	320
Copper	4.17 ± 0.03	0.272 ± 0.001	370
Nickel steel	3.98 ± 0.02	0.248 ± 0.001	200
Stainless steel	3.98 ± 0.08	0.237 ± 0.001	530

strongly weighted by the largest amplitudes in the histogram distribution and will be relatively insensitive to the smaller numbers associated with outliers. In this situation, no matter how many data are taken, the value of the simple average and the fitted peak position will never merge, and differences such as seen between values in Figure 5 and Table I are to be expected. Under these circumstances, it is expected that the position of the fitted peak will give a value closer to the true value, since the peak position is defined by the largest bin population.

An answer to the second question is more difficult and consists of two parts. First, if the skewed data reflect variations in the actual material properties, then an asymmetric distribution function, rather than a Gaussian, should be used to analyze the data. On the other hand, if the skewed distribution reflects artifacts in the data collection process, it may be legitimate to separate the skewed values from a symmetric scatter about the true value. If this is the case, how can the skewed contribution are removed from the data? To our knowledge, there is no straightforward mechanism to achieve this. However, review of Figure 5 shows that, with the single exception of the determination of H for Parylene C on the stainless steel substrate, there is no significant difference in E_r or H values for fits to the entire data sets and fits to the censored data sets. For the single exception, H for Parylene C on stainless steel, the uncertainty in the peak position, obtained from a fit to the complete data set, is so great that it results in a large proportion of nonphysical (i.e., negative) values in the H distribution. Therefore, it is assumed here that the censored data give a more accurate estimate of H for the stainless steel substrate.

On the basis of previous discussion, the values in Figure 5 are expected to be more accurate than those in Table I. However, the values for both E_r and H in Figure 5 clearly vary depending upon the substrate.

This would be expected for thin films but, at 16 μm, no effect of substrate modulus or hardness was expected with the penetration depths that were used. Because Parylene C provides coatings conformal to the substrate, at least qualitatively, it was initially thought that the observed substrate dependence was due to variation in substrate surface structure. However, as Table III shows, the trends in E_r and H for Parylene C on the various substrates are not the same as the trend in average surface roughness S_a. Similar comparisons with other surface roughness parameters (i.e., skewness, kurtosis, maximum peak height, maximum valley depth, and root mean square slope) also resulted in no correlation with either E_r or H. However, work describing the effect of certain substrates on the inhibition of Parylene deposition[6] did show a strong correlation between E_r values and the relative ease of Parylene C deposition on aluminum, copper, and iron-containing substrates. In that article, any iron-containing substrate showed a strong tendency to inhibit Parylene C deposition. Aluminum substrates showed no such tendency and copper substrates exhibited only a small tendency. Equally important, the authors postulate that coating formation eventually occurs on the Parylene-inhibiting substrates through the formation of isolated Parylene islands that eventually coalesce. This is in contrast to the postulated smooth, conformal coatings that form on aluminum and copper. While 16 μm is a thick coating for substrate chemistries to penetrate, the qualitative difference in deposition processes on the different substrates may be the source of the observed E_r variability.

In contrast to E_r, the substrate dependence of H does not mimic the substrate dependence shown previously[6] any more than it reflects any of the surface statistics. At this point, no potential source for the behavior shown in Figure 5 is postulated. Nevertheless, the data in Figure 5, which derive from two measured areas on each of two separate substrates as well as fits using censored and uncensored data, are highly reproducible and have small standard deviations. Consequently, it is assumed that the observed trend reflects a true substrate effect that is independent of surface topography.

Only two sets of published mechanical reference values were found for comparison to the present work. Lee and Cho reported $E_r = 3.1$ GPa and $H = 0.130$ GPa.[12] For that work, the substrate may have been glass. On the basis of ASTM test method D882,[13] SCS coatings cited a secant modulus of 2.8 GPa,[4] which corresponds to an E_r of 3.3 GPa, assuming $E_n \gg E_s$ and Poisson's ratio $\nu = 0.4$ for Parylene C.[7] The discrepancy between previous values and those obtained in the present study may reflect viscoelastic effects. Viscoelastic behavior will result in an initial unloading slope S that is artificially high due to material creep.[14] The coatings were tested at room temperature, below any reported value of T_g that the authors could find; none of the unloading curves exhibited the "nose" shape attributed to creep;[14] and all tests were made in a region that was known to be insensitive to P_{max} and unloading rate (Figures 1 and 2). Nevertheless, Parylene C is a polymer, and a certain amount of creep is expected to occur under the indenter tip, leading to somewhat elevated values of E_r and H. However, the indentations provide an appropriate tool for assessing the uniformity of the coatings on a given substrate and the variability of coating properties for different kinds of substrates.

Similar to the lack of hardness and elasticity data, there is a scarcity of quantitative experimental work supporting the assumption that Parylene C is conformal. The results of this study indicate that a more precise definition of that term is required. Reductions in S_a and S_{dq} showed that all surfaces became smoother and flatter after the metals were coated, indicating that the polymer coating is not perfectly conformal. Moreover, slope values calculated successively in the direction of the line scans at 1770 nm intervals were significantly different at the surface of the coating than at the surface of the bare metal.

These data also indicated that the extent of smoothing was both a function of initial surface roughness and substrate composition. For example, Table II shows that Parylene C coating reduced S_a measurements of aluminum and copper by 0.12 and 0.28 μm, corresponding to reductions of 27% and 43%, respectively. These differences reflect neither a consistent proportional nor an absolute change relative to bare substrate roughness measurements. In addition to the good reproducibility of the E_r and H results, changes in roughness and slope after coating provide additional evidence that substrate chemical composition has an effect on the deposition and polymerization processes and the corresponding degree of conformality.

CONCLUSIONS

Nanoindentation and profilometry were used to examine mechanical properties and surface roughness of 16 μm thick Parylene C coatings applied to mill-finished samples of aluminum, copper, nickel steel, and stainless steel. Elasticity and hardness results were positively skewed for all substrates. Profilometry results also indicated that coatings were smoother and flatter than their underlying substrates, which means that the film thickness was not entirely uniform, i.e., not strictly conformal.

The implications of these findings are potentially significant for coating of implantable medical devices. Because it has been shown that the Parylene C coatings are measurably not conformal, it follows that thicknesses are not consistent everywhere. Presuming that the polymer is structurally homogeneous, bio fluid and/or ionic transport rates would be greater through thinner areas than thicker ones, for example. Moreover, it is possible that the coating's surface roughness is a reflection of variable polymerization processes, which might further affect transport properties. These deviations from ideality must be properly characterized in order to reliably predict the barrier effectiveness of Parylene C *in vivo*.

It was concluded that fitting a symmetric Gaussian curve to the data more accurately modeled the true means than taking a simple average of all the data. Resulting average E_r for aluminum and copper were similar at 4.2 GPa, as were those of the steel samples at 4.0 GPa. There were not similar pairings for hardness values, which ranged from 0.24 to 0.27 GPa. These results also showed that despite very similar surface roughnesses, resulting values of E_r and H were statistically different for different substrate materials. This indicated that chemical composition of a surface, in addition to its mechanical finish, influenced the deposition-polymerization process of Parylene C. Viscoelastic effects undoubtedly compose an important component of the measured mechanical properties of Parylene C and are currently under investigation.

ACKNOWLEDGMENTS

A portion of this work was supported by the Research Associateship Programs Fellowships Office of the National Research Council.

REFERENCES

1. Licari, J. J. In Coating Materials for Electronic Applications: Polymers, Processes, Reliability, Testing; Andrew, W., Ed.; Noyes Publication: Norwich, NY, **2003;** Chapter 20, p 159.
2. Stark, N. *Med. Plast. Biomater. Magaz.* **1996,** *3*, 30.
3. Fortin, J. B.; Lu, T. M. In Chemical Vapor Deposition Polymerization: The Growth and Properties of Parylene Thin Films; Kluwer Academic Publishers: New York, **2004;** Chapter 1, p 4.
4. Specialty Coatings Systems. SCS Parylene Properties, Specialty Coatings Systems: Indianapolis, **2008;** p 5.
5. Oliver, W. C.; Pharr, G. M. *J. Mater. Res.* **1992,** *7*, 1564.
6. Vaeth, K. M.; Jensen, K. F. *Chem. Mater.* **2000,** *12*, 1305.
7. Harder, T. A.; Yao, T.-J.; Qing, H.; Shih, C.-Y.; Tai, Y.-C. In The Fifteenth IEEE International Conference on Micro Electro Mechanical Systems, Las Vegas, NV, January 20–24, 2002; Institute of Electrical and Electronics Engineers: Piscataway, NJ, **2002;** pp 435–438.
8. Senkevich, J. J.; Desu, S. B. *Polymer* **1999,** *40*, 5751.
9. Noh, H. S.; Moon, K. S.; Cannon, A.; Hesketh, P. J.; Wong, C. P. In Proceedings of the 54th Electronic Components & Technology Conference, Las Vegas, NV, June 1–4, 2004; Institute of Electrical and Electronics Engineers: Piscataway, NJ, **2004;** pp 924–930.
10. Fischer-Cripps, A. C. Nanoindentation, 2nd ed.; Springer: New York, **2004;** Chapter 1, p 14.
11. Hay, J. L.; O'Hern, M. E.; Oliver, W. C. In Fundamentals of Nanoindentation and Nanotribology; Materials Research Society: Warrendale, PA, **1998;** Vol. 522, pp 27–32.
12. Lee, H.; Cho, J. In Proceedings of IMECE2005, International Mechanical Engineering Congress and Exposition, Orlando, FL, November 6–11, 2005; American Society of Mechanical Engineering: New York; **2005,** pp 279–283.
13. ASTM D882–10 Standard Test Method for Tensile Properties of Thin Plastic Sheeting; American Society for Testing and Materials: West Conshohocken, PA, **2010.**
14. Feng, G.; Ngan, A. H. W. *J. Mater. Res.* **2002,** *17*, 660.